

Unified description of charge and spin excitations of stripes in cuprates.

J. Lorenzana^a and G. Seibold^b

^a*SMC-INFM, ISC-CNR and Dipartimento di Fisica, Università di Roma “La Sapienza”, Piazzale Aldo Moro 2, I-00185 Roma, Italy*

^b*Institut für Physik, BTU Cottbus, PBox 101344, 03013 Cottbus, Germany*

Abstract

We study stripes in cuprates within the one-band and the three-band Hubbard model. Magnetic and charge excitations are described within the time-dependent Gutzwiller approximation. A variety of experiments (charge profile from resonant soft X-ray scattering, incommensurability vs. doping, optical excitations, magnetic excitations, etc.) are described within the same approach.

Key words: Firstkeyword, Secondkeyword, Thirdkeyword

PACS: 74.72.-h, 74.25.Gz., 71.45.Lr, 72.10.Di

1. Introduction

If the mechanism of high- T_c superconductivity is electronic, to understand the excitation spectrum is as important as to understand phonons was important to develop BCS theory. In this regard charge and spin inhomogeneous states, often found in strongly correlated systems, are interesting because they can support new collective modes, “electronic phonons”, that would not be present in a weakly interacting fluid. For example stripes in cuprates have many oscillatory modes that can couple with carriers and eventually lead to pairing and superconductivity or anomalous Fermi liquid properties.

Cuprates, unlike BCS superconductors, are unique and therefore their remarkable properties may well be rooted on details. For example a recent study shows that superconductivity in $\text{La}_{2-x}\text{Sr}_x\text{CuO}_4$ appears only when incommensurate low energy scattering parallel to the CuO bond is present and not, when the scattering is on the diagonals (at very low doping), or when the system is in a more conventional Fermi liquid phase at high doping[1], thus the excitation spectra must

be understood in detail. In the last years we have developed a method to compute collective excitations of inhomogeneous strongly correlated systems based on a time-dependent Gutzwiller approximation (GA), named GA+RPA[2,3,4,5,6].

Many theoretical descriptions of cuprates are suited for only one experiment. Here we show that within the same approach one can reproduce a variety of experimental features of $\text{La}_{2-x}\text{Sr}_x\text{CuO}_4$ in the charge and magnetic channel. Results in the one-band Hubbard model (1BHM) and the three-band Hubbard model (3BHM) are quite similar. We compare results from both models.

For the 3BHM we use the following LDA parameter set: $\epsilon_p - \epsilon_d = 3.3$ eV for the splitting between the diagonal energies of a hole in the copper d - and oxygen p orbital, $t_{pd} = 1.5$ eV ($t_{pp} = 0.6$ eV) for the p - d (p - p) hopping integral, $U_d = 9.4$ eV ($U_p = 4.7$ eV) for the repulsion between two holes on the same Cu (O) orbital and $U_{pd} = 0.8$ eV for the Cu-O repulsion[7]. For the 1BHM results reported here we use $t = 353.7$ meV for the nearest neighbor hopping, $U = 8t$ for the effective on-site repulsion, and $t' = -0.2t$ for the next-nearest neighbor hopping.

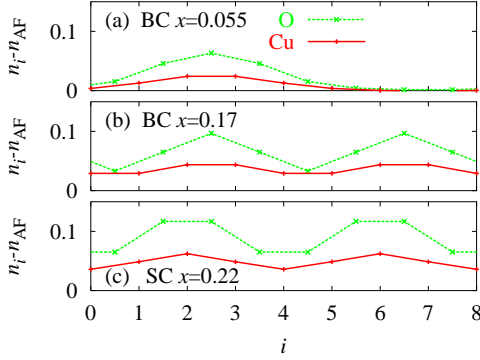


Fig. 1. Hole charge minus undoped charge in the 3BHM as a function of atomic position in the direction perpendicular to the stripes for various doping x , symmetry (BC or SC) and charge periodicity $d = 9$ (a); and $d = 4$ (b) and (c).

2. Ground state properties

Static properties are computed within the Gutzwiller approximation. Probes which are sensitive to the Cu and O atomic character need to be addressed with the 3BHM. In Fig. 1 we show the evolution of the charge profile with doping in the 3BHM for metallic stripes parallel to the CuO bond. The charge profile in real space has a width of about 4 lattice sites[8]. The width of the stripes defines two regimes: for low doping (a), the stripes do not overlap and therefore are weakly interacting, for high doping (b),(c) stripes overlap.

Recently Abbamonte and collaborators have shown that our charge profile predicted in the 3BHM[8] is in excellent agreement with the profile measured with resonant soft X-ray scattering[9].

The overall shape of the charge profile in the 1BHM is similar to the one in the 3BHM (see Ref. [10]). One also finds a non overlapping regime ($d > 4$), and an overlapping regime ($d \leq 4$).

For large and negative $-t'/t$ (non shown here) one finds that checkerboard states are favored[12].

In Fig. 2 we show the energy for metallic stripes as a function of doping for the 1BHM. In each curve the charge periodicity perpendicular to the stripe is fixed and takes integer values (from left to right) $d = 10 - 3$. In this computations stripes are bond-centered (BC). The energy for site-centered (SC) stripes is slightly lower at small doping but the differences decreases with the system size. At optimum doping both structures become degenerate.

A small difference with respect to the 3BHM is that in the latter BC stripes are more stable at low doping and become quasidegenerate with SC ones

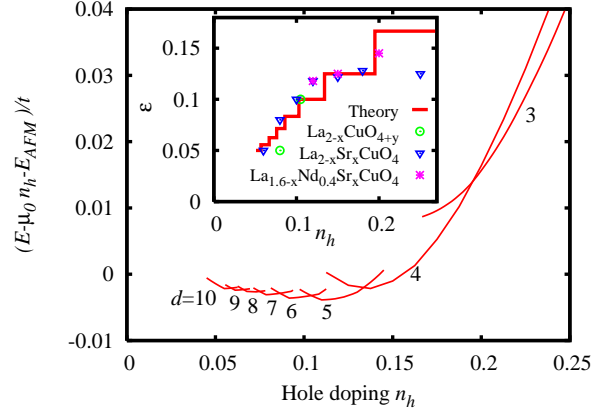


Fig. 2. Energy per site as a function of doping for stripes in the 1BHM. The curves are labeled by the charge periodicity d . For clarity we subtracted the energy of the AFM solution and the line $\mu_0 x$ with $\mu_0 = -1.6t$. Different choices of μ_0 correspond to different choices of the origin of the energy of the single particle states and do not change the physics. The inset reports the incommensurability as obtained from the present calculation (line) compared with experiment [11].

at optimum doping. Thus the role of SC and BC is interchanged. We expect the three-band results to be more reliable in this respect.

In the inset we plot the incommensurability vs. doping taking into account the range of stability of each solution and compared with experiments from Refs. [11]. The result is a Devil's staircase. Up to $x \approx 1/8$ the plateaux are short and correspond to a number of added holes per unit length along the stripe close to $\nu \sim 0.5$. As doping increases one jumps from one solution to the other and the density of stripes increases with doping. This explains the behavior of the incommensurability $\epsilon = 1/(2d) = x/(2\nu) \approx x$ as seen in neutron scattering experiments in this doping range. For $x > 1/8$ the right branch of the $d = 4$ solution is more stable than the $\nu \approx 0.5$ and $d = 3$ solution due to the overlap effect and one gets a wider plateau explaining the saturation of the incommensurability seen in the experiment.

Some details are slightly different in the 3BHM. The $\epsilon = 1/8$ plateau starts at lower doping and ends at higher doping improving the agreement with experiment[8]. For doping $x > 1/8$ holes populate the stripes and therefore the baseline in Fig. 1 increases.

For doping $x > 0.195$ ($x > 0.225$) in the one-band (three-band) model we find the $d = 3$ stripe ($\epsilon = 1/6 \approx 0.17$) to become the lowest energy solution. At this doping a variety of different solutions becomes close in energy and the present saddle-point

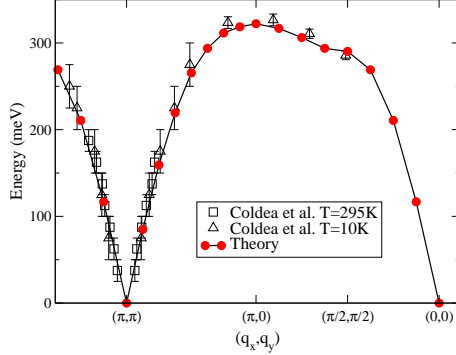


Fig. 3. Dispersion relation of the low-energy transverse excitations. We show the experimental result for La_2CuO_4 after Ref. [16] and the GA+RPA result.

approximation brakes down. Probably around this doping a quantum melting of stripes takes place.

It is also possible that the $d = 4$ stripe solution phase separates with the overdoped Fermi liquid skipping the $d = 3$ solution. This scenario will also produce a large $\epsilon = 1/8$ plateau in the incommensurate scattering. In this case long range Coulomb effects have to be taken into account[13].

One can see from the plot of the energy in Fig. 2 that the electron chemical potential $\mu = -\partial E/\partial x$ is approximately constant in the low doping regime (weakly interacting stripes) whereas it decreases in the overlapping stripe regime. The same behavior was found in a dynamical mean-field study of the one-band Hubbard model[14]. This is in qualitative agreement with experiment[15] although we find a larger rate of change of μ with doping than in the experiment. It is also possible that this is due to phase separation between $d = 4$ stripes and the overdoped Fermi liquid plus long-range Coulomb effects[13].

3. Magnetic excitations

The dispersion relation for magnetic excitations in the insulator computed within GA+RPA applied to the 1BHM are shown in Fig. 3 and is in excellent agreement with the experiment. The dispersion is weakly sensitive to t'/t and it is strongly sensitive to U/t . A larger U/t produces a flatter dispersion in the $(\pi, 0) - (\pi/2, \pi/2)$ direction which does not agree with the experiment[4].

The collective excitations in the stripe phase with the same parameter set have been reported in Ref. [5]. One obtains a resonance energy at 65 meV to be compared with the experimental value 55 meV[17]. A slight decrease of U improves the

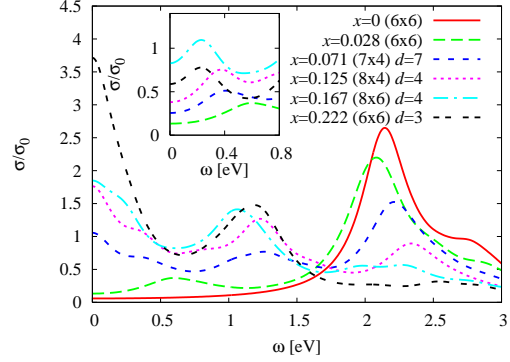


Fig. 4. Optical conductivity labeled by doping, system size and, in the case of stripes, interstripe distance. The units of conductivity are given by $\sigma_0 = 3.6 \times 10^2 (\Omega\text{cm})^{-1}$ with a background dielectric constant $\epsilon_b = 2.6$. The curve labeled $x = 0.028$ corresponds to the single-hole solution. For larger dopings the figure is an average over the electric field directions parallel and perpendicular to the BC stripes. The inset shows the MIR band excluding the Drude component. We used a Lorentzian broadening of 0.2eV.

agreement of the magnetic excitations with experiment as reported in Ref. [6] but produces a charge transfer gap in the insulator which is 10% too low. The present parameter set is a compromise between the charge and magnetic channel. Details of the magnetic response and the doping dependence are discussed in an accompanying paper[18].

4. Optical conductivity

The optical conductivity is qualitatively similar in the three-band and 1BHM. In Fig. 4 we show the result in the 3BHM. The charge transfer (CT) gap in the insulator is close to 2eV in good agreement with the experiment. In the 1BHM the CT gap is also at 2eV. This is mainly determined by our value of $U = 2.8\text{eV}$ confirming our parameter choice.

Doping induces a doping dependent mid-infrared (MIR) band and Drude weight at zero energy since our stripes are metallic. The MIR band is due to collective lateral fluctuations of the stripe. These lateral fluctuations form a band of excitations as for a violin string and the MIR band corresponds to the zero momentum component.

The “string” fluctuation band is massive due to pinning of the commensurate stripes to the underlying lattice. However, both the experiment[19] and our computations[3] show that the mass decreases with doping. This is rooted in the quasi-degeneracy found among BC and SC stripes and indicates that stripes form a floating phase at optimum doping.

Table 1

Selected excitations in meV in the one-band Hubbard model within the GA+RPA and in Experiment. Values marked with * are extrapolated.

	Momentum	x	Theory	Exp.	Ref.
CT gap	0	0	~ 2000	~ 2000	[19]
MIR band	0	0.08	~ 500	$\sim 250^*$	[19]
Magnon	$(\pi/2, \pi/2)$	0	293	286 ± 5	[16]
Magnon	$(\pi, 0)$	0	326	$333 \pm 7^*$	[16]
Resonance	0	1/8	65	55	[17]

The MIR band produces an absorption at low energy which explains the failure of the Drude model at optimum doping. This indicates that anomalous Fermi liquid properties are rooted in the low energy excitations of the floating phase.

In the 1BHM the MIR band is at energy ~ 0.5 eV for doping 0.08 which is higher than in the experiment (Table 1). Experimentally the band is located at ~ 0.5 eV at very low doping and softens with doping faster than what we found. This may be due to a finite size effect since our optical conductivity computations are done in system sizes much smaller than the computations of magnetic properties (16×4 and 40×40 respectively.)

Table 1 summarizes the energy of selected excitations in the 1BHM with the present parameter set. It is remarkable that such a simple model with only three parameters is able to provide a reasonable description of a variety of excitations in different channels plus several ground state properties.

5. Discussion and Conclusions

In cuprates true magnetic long-range order is sometimes detected in experiment[11] however, more often, Bragg peaks are not found. Two possibilities arise: the system may be close to a quantum critical point in the disordered phase (dynamic stripes) or the system may be in the ordered side of the transition but long-range order is not observed because of disorder (glassy stripes). Dynamic stripes have quasi long-range order in time and space whereas glassy stripes at low temperatures have practically long-range order in time but short range order in space as in a structural glass. This latter situation is clear for example in the magnetic channel at low doping, in muon spin-relaxation experiments where below a certain temperature the system develops a static (on the muon time scale) magnetic field which is not necessarily accompa-

nied by Bragg peaks[20], thus the spin rotational symmetry is broken without long range order. In these quantum or classically disordered cases our results apply as long as the energy scale is not too low (typically tenths of meV). How this reflects on the Fermi surface is discussed separately[21].

To conclude we have shown that the GA+RPA approximation allows for a unified description of collective modes in the charge and magnetic channel of striped cuprates. Results are similar in the one-band and the 3BHM although some details may differ in which case the 3BHM is expected to be more accurate. These modes are likely to play an important role in the anomalous properties of cuprates.

References

- [1] S. Wakimoto *et al.*, Phys. Rev. B 60 (1999) 769; Phys. Rev. Lett. 92 (2004) 217004.
- [2] G. Seibold, J. Lorenzana, Phys. Rev. Lett. 86 (2001) 2605; G. Seibold, F. Becca, J. Lorenzana, Phys. Rev. B 67 (2003) 085108; G. Seibold, F. Becca, P. Rubin, J. Lorenzana, Phys. Rev. B 69 (2004) 155113.
- [3] J. Lorenzana, G. Seibold, Phys. Rev. Lett. 90 (2003) 066404.
- [4] J. Lorenzana, G. Seibold, R. Coldea, Phys. Rev. B 72 (2005) 224511.
- [5] G. Seibold, J. Lorenzana, Phys. Rev. Lett. 94 (2005) 107006.
- [6] G. Seibold, J. Lorenzana, Phys. Rev. B 73 (14) (2006) 144515.
- [7] A. K. McMahan, J. F. Annett, R. M. Martin, Phys. Rev. B 42 (1990) 6268.
- [8] J. Lorenzana, G. Seibold, Phys. Rev. Lett. 89 (2002) 136401.
- [9] P. Abbamonte *et al.*, Nature Phys. 1 (2005) 155.
- [10] G. Seibold, J. Lorenzana, Phys. Rev. B 69 (2004) 134513.
- [11] J. M. Tranquada *et al.*, Nature (London) 375 (1995) 561; Phys. Rev. Lett. 78 (1997) 338; K. Yamada *et al.*, Phys. Rev. B 57 (1998) 6165.
- [12] G. Seibold, J. Lorenzana and M. Grilli, cond-mat/0606010.
- [13] J. Lorenzana, C. Castellani, C. Di Castro, Europhys. Lett. 57 (2002) 704.
- [14] M. Fleck *et al.*, Phys. Rev. Lett. 84 (2000) 4962.
- [15] A. Ino *et al.*, Phys. Rev. Lett. 79 (1997) 2101.
- [16] R. Coldea *et al.*, Phys. Rev. Lett. 86 (2001) 5377.
- [17] J. M. Tranquada *et al.*, Nature (London) 429 (2004) 534.
- [18] G. Seibold, J. Lorenzana, these proceedings.

- [19] S. Uchida *et al.*, Phys. Rev. B 43 (1991) 7942.
- [20] A. Keren, A. Kanigel, Phys. Rev. B 68 (1) (2003) 012507.
- [21] A. Di Ciolo *et al.*, these proceedings.